JOURNAL OF CATALYSIS 124, 52–72 (1990)

Conversion of Synthesis Gas over $LaMn_{1-x}Cu_xO_{3+\lambda}$ Perovskites and Related Copper Catalysts

J. A. BROWN BOURZUTSCHKY, N. HOMS,[1] AND A. T. BELL

Center for Advanced Materials, Lawrence Berkeley Laboratory; and Department of Chemical Engineering, University of California, Berkeley, California 94720

Received September 26, 1989 revised January 18, 1990

CO hydrogenation was investigated over perovskites with the composition $LaMn_{1-x}Cu_xO_{3+\lambda}$ (x = 0, 0.2, 0.4, 0.5, 0.6, 1.0); Cu supported on SiO_2, unpromoted and promoted with La_2O_3; Cu supported on La_2O_3 and on MnO_2/La_2O_3; and unsupported Cu metal powder containing traces of sodium (NaO_x/Cu). The $x = 0$ perovskite ($LaMnO_{3.24}$) was weakly active for CO hydrogenation and produced only hydrocarbons, whereas all other perovskites were more active and displayed >90% selectivity to alcohols (~80% methanol, ~10% C_{2+} alcohols). The C_{2+} alcohols followed a distribution characteristic of alkali-promoted copper catalysts. Cu/SiO_2 was >80% selective to hydrocarbons, and ≤5% selective to methanol. Introduction of La_2O_3 or NaO_x into the copper catalyst increased the CO hydrogenation activity and the selectivity to alcohols. The activities and product distributions of the Cu-containing perovskites ($x > 0$) are similar to those of NaO_x/Cu and the La_2O_3-containing catalysts, suggesting that the active sites in all of the catalysts are similar. It is proposed that hydrocarbon synthesis occurs at Cu^0 sites, but that Cu^0 and Cu^+ sites are required for the formation of methanol and C_{2+} alcohols. It is also proposed that Cu^+ sites are stabilized at the adlineation between metallic copper and lanthana (or soda).

INTRODUCTION

Copper/zinc oxide catalysts (Cu/ZnO) have been in use for the synthesis of methanol from CO and CO_2 under mild conditions ($P < 200$ atm, $T < 623$ K) since the inception of the ICI process in the 1960s (*1*). These catalysts are prepared coprecipitation methods and typically contain alumina or chromia for thermal stability. Structural and compositional analysis of copper/zinc oxide catalysts has revealed that the copper is present both as metallic copper particles and as Cu^+ ions dispersed in the zinc oxide (*2*). On the basis of extensive studies, Klier and co-workers (*2, 3*) have concluded that the Cu^+ ions are responsible for conversion of CO to methanol. They observed the methanol synthesis rate to be maximum in feeds containing small amounts of CO_2 and conclude that CO_2 helps maintain the active copper sites in the +1 oxidation state but is not a direct source for methanol (*3*). On the other hand, researchers at ICI (*4–8*) have proposed that the copper metal crystallites are the active phase, and that the surface of these crystallites is partially oxidized during reaction by adsorbed oxygen resulting from hydrogenation of CO_2. Using radiotracer techniques, they showed that in CO_2/CO mixtures, methanol is made directly from CO_2 rather than from CO and that the main function of CO is to scavenge the adsorbed oxygen to produce surface CO_2 (*4*).

It has been observed that the copper/zinc oxide system can be promoted with alkali metal, transition metal, or rare earth oxides to increase the methanol yield and/or shift the product distribution to include C_2–C_5 oxygenates (*9–15*). For example, promotion of a Cu/ZnO catalyst with K_2CO_3 increases its activity for methanol formation and enhances its selectivity for the formation of C_{2+}oxygenates, particularly ethanol

[1] Present address: Departament de Quimica Inorganica, Universitat de Barcelona, Av. Diagonal 647, 08028 Barcelona, Spain.

0021-9517/90 $3.00

and isobutanol (*11*). Other additives such as oxides of Cr, Mn, La, and Ce have been used in conjunction with alkali to give similar results (*12, 14*).

Zinc-free systems have also been studied. Owen *et al.* (*16, 17*) have investigated alloys of copper with various rare earth elements (Ce, La, Nd, Th). Exposure of these alloys to CO/H_2, produced a catalyst containing a bulk copper crystal phase and a rare earth oxide in which copper was highly dispersed. These catalysts were more active per unit surface area than $Cu/ZnO/Al_2O_3$ catalysts, particularly at temperatures below 523 K. The activity showed no correlation with the dispersion of the bulk copper phase and was instead attributed to the copper phase associated with the rare earth oxide. The authors suggested that this phase could be either ionic copper in the lanthanide oxide lattice or extremely small metallic particles.

Sheffer and King (*18*) have recently reported that promotion of an unsupported copper catalyst with potassium increases the activity for methanol formation from CO/H_2 almost tenfold. In a subsequent study, the same authors (*19*) reported that the activity of unsupported copper promoted with a group IA metal (Li–Cs) correlates linearly with the presence of Cu^+ ions at the catalyst surface. From results of NMR and XPS characterization, it was deduced that treatment of these catalysts with CO/H_2 created an alkali carbonate phase, and this was proposed to be responsible for stabilization of the Cu^+ ions.

The addition of group IA metals has also been found to enhance the formation of higher alcohols, particularly at low H_2/CO ratios (*10, 11, 20*). Results of an extensive study of the action of Cs on Cu/ZnO suggest that the base enhances the surface concentration of oxygen-containing intermediates (RCO^- and $RCOO^-$), thereby increasing the probability of these species reacting with adsorbed C_1 intermediates (HCO^- or H_2CO) to form longer chains (*10*). Xiaoding *et al.* (*21*) have suggested that basic promoters may suppress the hydrogenation activity of Cu/ZnO, thereby increasing chain growth relative to chain termination.

Copper-containing lanthanum perovskites have also been studied for oxygenate synthesis. Broussard and Wade (*22*) have noted that the substitution of Mn by Cu in $LaMnO_3$ shifted the product distribution from 100% hydrocarbons to significant amounts of methanol and small amounts of C_{2+} oxygenates. These authors concluded that Cu is the active metal for oxygenate formation and suggested that it exists at the catalyst surface in an oxidation state greater than zero, stabilized by the perovskite lattice.

The aim of the present study was to investigate the effects of lanthanum and manganese oxides on the activity and selectivity of Cu for CO hydrogenation. Three types of catalyst were investigated: (i) perovskites of the stoichiometry $LaMn_{1-x}Cu_xO_{3+\lambda}$ ($0 \leq x \leq 1$); (ii) Cu supported on SiO_2, unpromoted and promoted with La_2O_3; and (iii) Cu supported on La_2O_3 and on MnO_2/La_2O_3. For comparison, experiments were also carried out with unsupported copper powder. The catalysts were characterized by X-ray diffraction and X-ray photoelectron spectroscopy after use under reaction conditions to assess the state of Cu in the working catalyst. Either direct or indirect evidence was found for Cu^0 particles in the majority of the catalysts following use. The activity and selectivity of Cu were found to be strongly affected by the presence of lanthana. Lanthana present as either a support or a promoter increased the overall CO hydrogenation activity and shifted the product distribution from hydrocarbons to methanol and C_{2+} alcohols.

EXPERIMENTAL

Catalyst Preparation

A series of $LaMn_{1-x}Cu_xO_{3+\lambda}$ ($0 \leq x \leq 1$) perovskites were prepared as follows (*22*). $La(NO_3)_3 \cdot 6H_2O$, $Mn(NO_3)_2 \cdot 4H_2O$, and

$Cu(CH_3COO)_2 \cdot H_2O$ were mixed together in desired proportions to give a concentrated solution to which was added sufficient citric acid (monohydrate) such that the number of gram equivalents added equaled the total number of metal gram equivalents. The solution was evaporated at 343 K and 10 Torr to produce a viscous syrup and then evacuated further at 373 K for 5 h to produce a totally amorphous solid. This product was calcined at 973 K in He (99.998%) for 5 h, thereby effecting decomposition of the citrate complex (*23, 24*). For $x < 1$, calcination produced shiny black crystals which exhibited no change in color after reduction and use for CO hydrogenation. For $x = 1$, a dull black powder was obtained, which took on a reddish tinge after reduction. No further change in the color of this catalyst was observed after use.

Unsupported copper was prepared according to the method of Herman *et al.* (*2*). A solid precipitate was formed from a 1 *M* aqueous solution of $Cu(NO_3)_2 \cdot 3H_2O$ (Baker Chemical Co.) by dropwise addition of a 1 *M* aqueous solution of Na_2CO_3 (anhydrous, Mallinckrodt) under constant agitation, until the pH increased from 2.6 to 7.1. The temperature was held at 361 K throughout the entire process. Approximately 500 ml of the sodium carbonate solution was required to fully treat 500 ml of the copper nitrate solution. The slurry was cooled over 2 h to room temperature, then washed and filtered in batches before drying at 353 K in nitrogen at 1 atm. The resulting fine green powder was calcined in air by raising the temperature from 423 to 623 K in 50 K increments over a period of 2 h. The final temperature was held for 3 h, before cooling to 323 K. The black copper oxide so produced was ground to 30–60 mesh (600–246 μm) and stored in a desiccator until further use. After reduction the catalyst turned a shiny brick red color characteristic of copper metal. This color remained the same even after the catalyst had been used for a reaction.

A silica-supported copper catalyst was prepared by incipient wetness impregnation of amorphous silica (M-5, Cab-O-Sil, 250 m^2/g, Cabot Corp.) with an aqueous copper nitrate solution of the desired concentration. The resulting paste was dried at 125 Torr and 343 K for 10–15, ground, pressed, and sieved to yield granules of 30–60 mesh (600–246 μm). The entire catalyst batch was then calcined in air at 573 K for 3–4 h. Calcination was essentially complete in 2 h or less, at which point the light blue copper nitrate was entirely converted to black cupric oxide. After being cooled to 320 K in air, the batch was discharged and stored in a desicator until further use. Reduction produced a reddish-brown catalyst, the color of which was unchanged by reaction.

Lanthana-promoted copper/silica was prepared by impregnation of ground unreduced CuO/SiO_2 with an aqueous solution of $La(NO_3)_3 \cdot 6H_2O$ (Fisher Chemical Co.). The resulting gray paste was dried, pelletized, calcined, and stored, as described above for Cu/SiO_2. Upon calcination the catalyst turned black; reduction and use for reaction did not change the color.

Lanthana-supported copper catalysts were prepared as follows. La_2O_3 (99.9%, Union Molycorp) was hydrated by refluxing for 15 h at 343 K to increase its surface area (10.9 m^2/g) (*25, 26*). After being dried under vacuum at 353 K, the powder was impregnated gradually (over 5 days), with an aqueous copper nitrate solution of the desired concentration. The resulting blue paste was dried slowly at 343 K and 1 atm, as drying under vacuum tended to form a solid that was very difficult to grind. The catalyst was then sieved before calcination in air at 573 K. Upon calcination the catalyst turned black. No further change in the color of this catalyst occurred after reduction or use for CO hydrogenation.

The incorporation of manganese oxide was achieved by incipient wetness impregnation of hydrated lanthana with an aqueous solution of $Mn(NO_3)_2$ (50–52% aq., Baker Chemical Co.). The product was

then dried, sieved, and calcined at 723 K to ensure formation of MnO_2. The resulting gray pellets were ground, then impregnated with copper nitrate and treated as described above for Cu/La_2O_3. Upon calcination the color did not change, but reduction and use for reaction produced a reddish-gray color. While the presence of stoichiometric MnO_2 could not be identified, the catalysts containing manganese oxide on lanthana are designated as $Cu/MnO_2/La_2O_3$ for the sake of convenience.

Catalyst Characterization

The perovskite catalysts were characterized by X-ray diffraction after oxidation, after reduction, and after use for CO hydrogenation. Characterization of the oxidized and reduced samples was performed on a Phillips Model PW 1716/30 diffractometer, whereas characterization of the samples after use for catalysis was performed on a Siemens Model D-500 diffractometer. The oxygen content of the oxidized perovskites was determined by TPR/TGA analysis (*23*). XPS analysis of the perovskites after reaction was carried out on a PHI Model 5300 ESCA spectrometer. Integrated areas for the observed lines were adjusted by the sensitivity factors recommended by the manufacturer (*27*) and used to calculate surface atomic ratios. The BET surface area of the oxidized perovskites was determined by N_2 adsorption.

The metal contents of the supported catalysts and of the unsupported copper powder were determined by atomic absorption spectrometry and by X-ray fluorescence wherever possible. The BET area of these catalysts was determined by N_2 adsorption. All catalysts were characterized after reaction using XRD and XPS, to determine their bulk structure and surface composition, respectively.

Determination of the copper metal surface area for the supported copper catalysts proved to be difficult. Attempts to use O_2 adsorption at 77 K according to the method described by Parris and Klier (*28*) gave irreproducible and unreasonable values, i.e., ones that implied the available surface copper to be three orders of magnitude greater than the total amount of copper in the catalyst. Consequently, it was decided to use CO chemisorption. The stoichiometry of CO adsorption was determined by first measuring the N_2 BET isotherm of reduced unsupported copper at 77 K. A CO isotherm, measured on the same sample at 298 K, was then compared to the BET area to yield a calibration value of 5.06 μmol CO/m^2 Cu, or $\theta = 0.18$ monolayer, assuming 1.7×10^{19} atoms Cu/m^2 Cu (*29*). This value agrees well with previous work: Parris and Klier (*28*) obtained $\theta = 0.18$ for CO chemisorption and Dell *et al.* (30) obtained values in the range $\theta = 0.2$–0.25. CO isotherms of the silica-supported catalysts were measured after reduction, and again after use and rereduction. After measurement of the first isotherm, the sample was evacuated at 298 K for up to 12 h and then exposed again to CO at 298 K. No CO was taken up under these conditions, indicating that evacuation at 298 K did not remove the initially adsorbed CO. However, evacuation at 423 K for 10 h or more was found to restore the original CO uptake capacity. For the lanthana-containing catalysts, it was not possible to determine the Cu metal area since lanthana adsorbs CO with unknown stoichiometry. With use, the copper area of Cu/SiO_2 was reduced to almost half of its original value, whereas the area of unsupported copper was essentially unchanged.

Catalytic Testing

All tests of catalytic activity were carried out in a stainless-steel microreactor (6.4-mm i.d.) heated by a tube furnace. The reaction pressure was maintained by means of a back-pressure regulator, in the range of 7.5–14 atm. The reactants were supplied from a pressurized manifold via individual flow controllers. Carbon monoxide (UHP, Matheson) was purified further by passage through a column of glass beads maintained

at 388–400 K and a subsequent column of molecular sieves at 298 K. Hydrogen (UHP, Matheson, and Amerigas, 99.999%) was purified by passage through a catalytic oxygen remover (Matheson Model OR-10-641010). This unit consists of a column of platinum catalyst, which converts any oxygen in the hydrogen to water. The water is then removed upon passage through a column of molecular sieves at room temperature (298 K).

The reactor effluent was analyzed by gas chromatography using a Varian Model 3700 GC, equipped with an automated on-line gas sampling valve maintained at 434 K. The transfer line between the reactor and the valve was Teflon lined and kept above 397 K to eliminate any product loss due to absorption and/or condensation. Blank runs performed with an empty reactor showed no evidence of product formation.

Methanol, CO_2, and H_2O were separated using a 1.83-m-long, 2.16-mm-i.d. column packed with Chromosorb 107 (80–100 mesh) and connected to a TCD. The column temperature was held at 303 K for 2 min after sample injection and then raised at 25 K/min to a final temperature of 493 K. Quantitative analysis of all organic products was achieved using a 1.83-m-long, 2.16-mm-i.d. column packed with Porapak PS and connected to a FID. The column temperature was held at 303 K for 2 min following sample injection, and then increased at 15 K/min to a final temperature of 413 K. By this means resolution was achieved of C_1–C_7 hydrocarbons and C_1–C_4 oxygenates. Paraffins and olefins could not be resolved beyond C_4.

The procedure used to evaluate catalytic activity was the same for all catalysts. Typically, 0.5–2 g of catalyst was charged into the reactor. A flow of H_2 was then passed through the reactor at 80 ml/min/g catalyst and the temperature raised to the desired reduction temperature at a rate of 4–8 K/min. Throughout reduction, the evolution of water in the reactor effluent was monitored by gas chromatography. Reduction conditions were maintained for 2 h beyond the point where no further water could be detected, before initiating reaction. To initiate reaction, the temperature and pressure were set to desired values; then the H_2 flow was adjusted and the CO flow introduced to give the desired partial pressures. After a break-in time of about 15 h on stream, the first data point was taken. Following a change in reaction conditions, 2–4 h was allowed for the catalyst to come to steady state. Repetition of the initial conditions after 1–2 weeks of testing showed little deactivation of any of the catalysts.

RESULTS

Catalysts Characteristics

The composition and physical characteristics of the catalysts used in this study are listed in Table 1. The BET areas for the perovskites lie in the range 7–25 m^2/g. The BET surface areas of the lanthana-supported catalysts are also in this range but those for the silica-supported catalysts are much higher, reflecting the BET area of the silica (250 m^2/g). The Cu surfaces areas for Cu powder and Cu/SiO_2 are similar in magnitude. The copper surface area reported for lanthana-promoted Cu/SiO_2 is based on the assumption that the Cu particle sizes for the promoted and unpromoted catalysts are equivalent. This assumption is supported by both XPS and XRD observations.

Examination of the perovskites by XRD prior to reduction and use revealed the presence of a single orthorhombic perovskite phase in all but one case (*23*). This exception was for $x = 1$, in which case La_2CuO_4 and CuO were found.[2] The oxygen stoichiometry (λ) of the calcined

[2] This catalyst is thought to consist of layers of perovskite sheets of $LaCuO_3$, each separated by a layer of LaO; however, the catalyst is referred to as the "$x = 1$ perovskite" for the sake of convenience. $LaCuO_3$ as a single perovskite phase has been made (*31*), but is unstable. In the present case it is believed that during calcination, the oxygen-deficient perovskite $LaCuO_{2.5}$ formed, then disproportionated into La_2CuO_4 and CuO (*23*).

TABLE 1

Catalyst Characteristics

Catalyst	BET area (m^2/g)	Crystallite size[a] (Å)	Cu area [b] (m^2 Cu/g)
$LaMnO_{3.24}$	11.0	—	—
$LaMn_{0.8}Cu_{0.2}O_{3.13}$	17.1	—	—
$LaMn_{0.6}Cu_{0.4}O_{3.14}$	24.5	—	—
$LaMn_{0.5}Cu_{0.5}O_{3.00}$	17.8	—	—
$LaMn_{0.4}Cu_{0.6}O_{2.93}$	21.4	—	—
$LaCuO_{2.69}$ (= La_2CuO_4 + CuO)	6.6	—	—
NaO_x/Cu powder (0.3 wt% Na)	0.7	230	0.13
Cu/SiO_2 (9.3 wt% Cu)	258.0	250	0.08
$La_2O_3/Cu/SiO_2$ (2.1 wt% La, 8.6 wt% Cu)	205.0	240	{0.08}[c]
Cu/La_2O_3 (9.8 wt% Cu)	11.9	~100	—
$Cu/MnO_2/La_2O_3$ (9.6 wt% Cu, 12.3 wt% Mn)	6.3	330	—

[a] Determined from FWHM of Cu(111) XRD line.
[b] Based on CO chemisorption.
[c] Taken as intrinsic copper area, i.e., that of Cu/SiO_2 if no lanthana were added.

perovskites was determined by TPR/TGA as follows. Each catalyst was subjected to temperature-programmed reduction up to 973 K. The reduced catalyst was then analyzed by XRD and found to contain only La_2O_3, MnO, and Cu metal (La_2O_3 and MnO in the case of $LaMnO_{3.24}$). The observed weight loss was ascribed to loss of oxygen from the lattice and catalyst surface. Assuming the metal atomic ratios to be those of the original preparation, the oxygen content of the final products was calculated. Combining this with the oxygen removed by reduction gave the total amount of oxygen present in the unreduced sample.

Table 1 shows that as x increases, the oxygen content (λ) decreases, reflecting the substitution of Mn^{3+} and Mn^{4+} by Cu^{2+}. This results in an increased number of oxygen vacancies in the perovskite lattice, making it less stable and easier to reduce. Thus at $x = 1$, calcination produces the more stable mixed oxide La_2CuO_4 instead of the perovskite $LaCuO_3$, and the excess copper forms CuO. Rojas *et al.* (*23*) also observed that under reducing conditions, the perovskites with $x \leq 0.6$ maintain the lattice structure at temperatures as high as 800 K. For $x = 1$, reduction below 500 K reduces CuO to Cu metal but La_2CuO_4 is unaffected; reduction above 600 K produces copper metal and lanthana.

The two perovskites for which $x = 0.2$ and $x = 1$ were investigated by XRD after reduction at two different temperatures and use for reaction. The XRD patterns of the $x = 0.2$ perovskite reduced at 573 and 723 K showed the structure of each sample to be the same as that of the fresh catalyst. XRD of the used $x = 1$ perovskite reduced at 523 K revealed the presence of La_2CuO_4 and metallic copper, whereas a sample reduced at 723 K was found to contain only metallic copper and a mixture of lanthanum species such as $La(OH)_3$ and $La_2(CO_3)_3$. The FWHM of the Cu^0 lines in the diffraction pattern for the sample reduced at 723 K were narrower than those in the sample re-

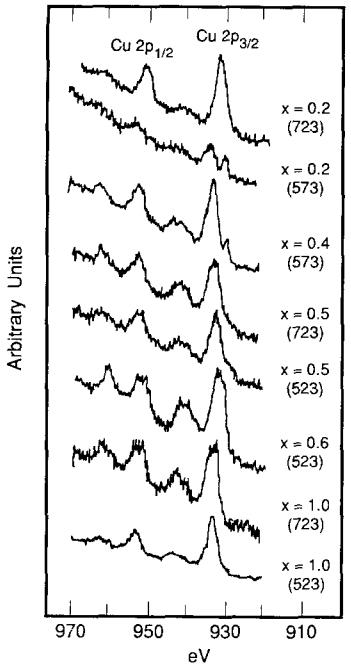

FIG. 1. X-ray photoelectron spectra of the spent perovskites $LaMn_{1-x}Cu_xO_3$: Cu 2*p* region. Catalysts reduced at the temperature shown in parentheses. Spectra taken after transfer in air. Peak positions referenced as described in Table 2a.

duced at 523 K, indicative of a lower dispersion.

Microchemical analysis of copper powder revealed that sodium was present on the order of 0.3 wt% in the catalyst after reduction and use for reaction. The presence of Na in the catalyst surface was confirmed by XPS (see below) and is doubtless a remainder of the Na_2CO_3 precipitant used in the preparation. For comparison, sodium was not found in the surface of Cu/SiO_2.

The size of the Cu crystallites for the silica-supported catalysts and copper powder are close in magnitude, lying in the range 230–250 Å, whereas $Cu/MnO_2/La_2O_3$ has a larger crystallite size of ~330 Å. For Cu/La_2O_3 the copper lines in the diffraction pattern were very broad and of low intensity. The crystallite size is estimated to be on the order of 100 Å, indicating that the copper dispersion is almost three times greater for this catalyst compared to that of the others. The XRD patterns for $La_2O_3/Cu/SiO_2$ and $Cu/MnO_2/La_2O_3$ showed no evidence for La_2O_3 or MnO_2, respectively. This implies that the dispersed metal oxide in both cases is present as particles smaller than 30–50 Å.

Figure 1 shows the Cu 2*p* region of the X-ray photoelectron spectra for the perovskite catalysts. The binding energies for Cu and Mn and the ratios of Cu/La and Mn/La are reported in Table 2a. The corresponding information for the remaining catalysts is presented in Fig. 2 and Table 2b. All of the binding energies listed in Tables 2a and 2b are referenced to the $3d_{5/2}$ peak of lanthana at 834.9 eV or are as noted in the tables. Identification of the oxidation state of copper was complicated by the fact that the binding energies for Cu^0 and Cu^+ are essentially the same and differ from that for Cu^{2+} by ~1.5 eV. Cu^{2+} can be distinguished, however, by the presence of

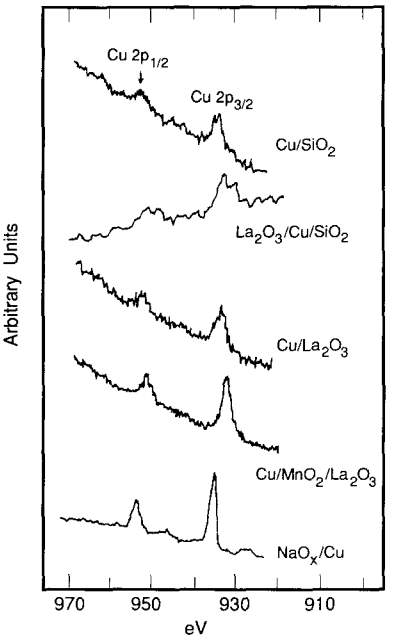

FIG. 2. X-ray photoelectron spectra of spent copper catalysts: Cu 2*p* region. All catalysts reduced at 573 K. Spectra taken after transfer in air. Peak positions referenced as described in Table 2b.

TABLE 2a

XPS Results: Perovskites[a]

Catalyst	Binding energy (eV)		Surface atomic ratio	
	Cu	Mn	Cu/La	Mn/La
$LaMnO_{3.24}$ (573, 723 K)	—	642.0	0.00	0.79
$LaMn_{0.8}Cu_{0.2}O_{3.13}$ (723 K)	932.2	640.7	0.32	0.46
$LaMn_{0.8}Cu_{0.2}O_{3.13}$ (573 K)	934.0	642.0	0.09	0.54
	930.0	(23% total Cu)		
$LaMn_{0.6}Cu_{0.4}O_{3.14}$ (573 K)	933.3	641.5	0.56	0.38
	929.9	(10% total Cu)		
$LaMn_{0.5}Cu_{0.5}O_{3.00}$ (723 K)	933.1	641.2	0.46	0.16
$LaMn_{0.5}Cu_{0.5}O_{3.00}$ (523 K)	932.8	641.6	0.47	0.22
$LaMn_{0.4}Cu_{0.6}O_{2.93}$ (523 K)	932.1	641.5	0.64	0.18
$LaCuO_{2.69}$ (723 K)	932.6	—	1.11	—
$LaCuO_{2.69}$ (523 K)	932.7	—	0.71	—

[a] Data taken after reduction at the temperature in parentheses and subsequent reaction. Binding energies referenced to La 3*d* at 834.9 eV.

shake-up satellite peaks ~10 eV above the major lines in the Cu 2*p* region of the spectrum.

The Cu 2*p* region of the X-ray photoelectron spectrum of all the perovskites (x = 0.2–0.6) displays shake-up satellites, giving evidence for the presence of Cu^{2+}. TPR and XPS characterization of these catalysts by Rojas *et al.* (*23*) suggests that, under the conditions used in the present study, the copper in these catalysts would be reduced to either Cu^+ or Cu^0. The XPS results presented in Fig. 1, however, indicate that the copper is only partially reduced. The binding energies for the Cu $2p_{3/2}$ peak all lie within 1.8 eV of each other and show no trend with increasing values of x.

The X-ray photoelectron spectra for the two samples of the x = 1 perovskite also show shake-up satellites, attesting to the presence of Cu^{2+} ions in the catalysts after reduction and use. However, in contrast to

TABLE 2b

XPS Results: Copper Catalysts[a]

Catalyst	Binding energy (eV)		Surface atomic ratio		
	Cu	Mn	Cu/La	Mn/La	Cu/Si
Cu/SiO_2	933.1	—	—	—	0.019
$La_2O_3/Cu/SiO_2$[b]	932.0	—	—	—	0.018
	929.2	(40% total Cu)			
Cu/La_2O_3	932.5	—	0.21	—	—
$Cu/MnO_2/La_2O_3$	931.1	645.8	0.25	0.108	—
NaO_x/Cu powder	934.2	(Na: 1072.7 eV)		(Na/Cu ≈ 0.11)	

[a] After reduction at 523 K and use for reaction. Error in BE is ~1 eV. Data referenced to Si 2*p* (103.4 eV) for silica supported catalysts, to La $3d_{5/2}$ (834.9 eV) for lanthana-supported catalysts, to unaltered for Cu powder.

[b] No La signal observed for this sample.

the other perovskite catalysts, XRD clearly indicates the presence of Cu^0 crystallites in both samples. The existence of metallic copper in the catalysts used is also suggested by their reddish tint, which contrasts with the color of the other perovskites, which all remain black. For the sample reduced at 523 K, the presence of Cu^{2+} in the La_2CuO_4 phase is expected; however, as reduction at 723 K eliminates both CuO and La_2CuO_4 (see XRD results above), the Cu^{2+} in this catalyst must exist only at the surface.

The surface atomic ratios of the perovskites (Table 2a) generally follow the trend of the bulk composition; i.e., the Cu/La ratio increases with x. For $x = 0.2$ and 1 the Cu/La ratio was higher for samples reduced at 723 K than at 523 K, whereas for $x = 0.5$ the ratio barely changed.

Figure 2 shows the Cu 2*p* region of the X-ray photoelectron spectra of the supported catalysts and copper powder, taken after use and exposure to air. None of the spectra contain shake-up satellites, indicating that Cu^{2+} ions are not present in any of the catalysts. Since the XRD pattern of the spent catalyst indicates Cu^0 crystallites to be present in all cases, the Cu $2p_{2/3}$ lines seen in Fig. 2 are attributed primarily to Cu^0. However, as discussed below, the possible presence of Cu^+ ions cannot be ruled out completely.

The Cu/La surface atomic ratios of the lanthana-supported catalysts are closest to the values for the $x = 0.2$ perovskite, although the latter catalyst has a lower bulk copper content. It was not possible to obtain a Cu/La ratio for $La_2O_3/Cu/SiO_2$, as no bands for La 3*d* could be discerned in the X-ray photoelectron spectrum of this catalyst. This suggests that lanthanum constitutes 1% or less of the catalyst surface. The Mn/La ratio of $Cu/MnO_2/La_2O_3$ is similar to that of the $x = 0.6$ perovskite. The BE for Mn in $Cu/MnO_2/La_2O_3$ is very high compared to those for the perovskites. This could be due to differences in catalyst formulation and, hence, differences in the electronic environment and oxidation state of the manganese ion. $Cu/MnO_2/La_2O_3$ was reduced at 523 K, which is not sufficient to begin reduction of MnO_2 (*23*).

For four catalysts (the $x = 0.2$ and $x = 0.4$ perovskites, $La_2O_3/Cu/SiO_2$, and copper powder) a second XPS band for copper can be seen, ~4 eV below the major line. Interaction of copper with lanthana, e.g., electron donation, may result in a more electronegative copper species and a decrease in binding energy of copper electrons. This explanation can also apply to the NaO_x/Cu catalyst for copper in the neighborhood of sodium. Similar effects have been observed for such catalysts as Pd/La_2O_3 and copper powder promoted with lithium. In a study of Pd/La_2O_3, Hicks *et al.* (*32*) found the BE for Pd 3*d* in Pd/La_2O_3 catalyst to be generally 0.1–0.9 eV lower than the BE value for either metallic Pd or Pd in Pd/SiO_2. In these catalysts, partially reduced LaO_x species are believed to be closely associated with the Pd phase, and the decrease in BE was attributed to electron donation from these lanthanum species to the Pd centers. Similarly, Sheffer and King (*19*) have found that the Cu 2*p* binding energy in Li-promoted copper powder is 1.5 eV below that of unpromoted copper and attribute this to electron donation from lithium to copper.

As noted earlier, it was not possible to discern lanthana in $La_2O_3/Cu/SiO_2$ by XRD or XPS. However, the presence of lanthana is suggested by simple visual observation. After reaction unpromoted Cu/SiO_2 is red, whereas $La_2O_3/Cu/SiO_2$ remains black. Similarly, Cu/La_2O_3 and the perovskites for which $x \leq 0.6$ were also black, whereas $Cu/MnO_2/La_2O_3$ and the $x = 1$ perovskite were tinged with red after reduction and use for reaction. The most likely source of the black color is ionic copper dispersed in the lanthana. Herman *et al.* (*2*) have noted that cationic substitution of Cu^+ into ZnO

causes the Cu/ZnO catalysts to be black, even though ZnO is white and metallic copper is red. It would appear, therefore, that a portion of the copper in $La_2O_3/Cu/SiO_2$ and Cu/La_2O_3 is present in the lanthana lattice. In the case of $La_2O_3/Cu/SiO_2$, it is possible that during impregnation of CuO/SiO_2 with aqueous lanthanum nitrate, some of the CuO dissolves into the liquid phase, and precipitates with the $La(NO_3)_3$ upon drying. Calcination would then result in a mixed oxide phase in which copper (oxide) is incorporated into lanthana (e.g., as $LaCuO_n$). For the $x \leq 0.6$ perovskites, copper is expected to be atomically dispersed in the crystalline perovskite lattice. The $x = 1$ perovskite is not actually a perovskite lattice, but is instead a mixture of La_2CuO_4 and copper oxide. Reduction has been shown to produce crystalline copper metal, which probably accounts for the observed reddish color.

Activity

The activities of the perovskite and lanthana-supported catalysts are listed in Table 3a for a range of experimental conditions. In each case, the activity is expressed on the basis of the BET surface area. For a given set of reaction conditions the activity of the perovskites increases with increasing values of x up to $x = 0.5$, then decreases slightly before rising to a maximum at $x = 1$. This variation is actually not very great, as can be seen from Fig. 3, in which activity is plotted against the mole fraction of Cu. The lanthana-supported catalysts are included in Fig. 3 since the composition and BET areas of these catalysts are similar to those of the perovskites. It is apparent that the lanthana-supported catalysts have activities comparable to those of the perovskites. The activity of $Cu/MnO_2/La_2O_3$ is lower than that of Cu/La_2O_3 and is not very different from that of the $x = 0.4$ perovskite, the perovskite closest in composition to $Cu/MnO_2/La_2O_3$.

Table 3b reports the activities of the copper powder and the silica-supported catalysts calculated on the basis of copper surface area. For $H_2/CO = 2$, the activity of

TABLE 3a

Activity of Perovskites and Lanthana-Supported Catalysts[a]

	Rate (μmol CO converted/min/m^2 catalyst)[b]				
P (atm)	7.4	10.6	10.6	10.6	13.8
H_2/CO[c]	1	2	2	2	3
T (K)	573	573	523	498	573
Perovskites					
$x = 0$	0.068	0.082	—	0.002	0.12
$x = 0.2$	0.095	0.17	0.042	0.01	0.18
$x = 0.4$	0.47	0.85	0.31	0.12	1.09
$x = 0.5$	0.79	1.45	0.98	0.40	2.06
$x = 0.6$	0.56	0.97	0.44	0.23	1.44
$x = 1$	0.96	1.69	0.62	0.32	2.47
Cu/La_2O_3	—	1.20	—	—	—
$Cu/MnO_2/La_2O_3$	—	0.75	—	—	—

[a] Perovskites $x = 0$, 0.2, and 0.4, reduced at 573 K. All other catalysts reduced at 523 K.

[b] Conversion of CO to organic compounds only.

[c] $F/W \approx 200$ ml/min/g catalyst.

TABLE 3b

Activity of Copper Catalyst Specific to Cu Area[a]

	Rate (μmol CO converted/min/m_2 Cu)[b]				
P (atm)	7.4	10.6	10.6	10.6	13.8
H_2/CO[c]	1	2	2	2	3
T (K)	573	573	523	498	573
NaO_x/Cu	—	18.38	2.55	1.00	28.22
Cu/SiO_2	—	11.05	3.94	1.27	11.38
$La_2O_3/Cu/SiO_2$	31.05	46.61	23.27	4.11	54.33

[a] Catalysts reduced at 523 K.
[b] Conversion of CO to organic compounds only.
[c] $F/W \simeq 60$ ml/min/g catalyst.

the copper powder decreases more rapidly than that of Cu/SiO_2 with decreasing temperature. Lanthana promotion of Cu/SiO_2 increases the catalyst activity at all temperatures.

Product Distribution

C_1–C_4 alkenes, alkanes, and alcohols were the principal organic products formed over each catalyst. Among the hydrocarbons, methane was the dominant product (>50% on a carbon atom basis), with ethane and propane making up most of the balance of this fraction. CO_2 was detected in the products but no evidence of H_2O was found for any of the catalysts.

Table 4a lists the product distribution observed under a fixed set of reaction conditions for each catalyst. $LaMnO_{3.24}$ produces only hydrocarbons in an Anderson–Schulz–Flory distribution characterized by a chain growth probability $\alpha = 0.54$. Upon

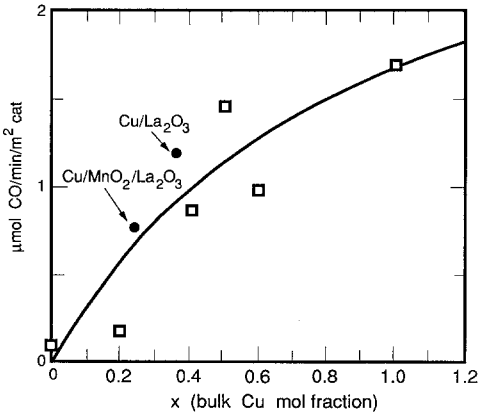

FIG. 3. Correlation of CO hydrogenation activity with bulk Cu mole fraction, for perovskites and lanthana-supported catalysts ($H_2/CO = 2$, $P = 10.6$ atm, $T = 573$ K).

TABLE 4a

Product Distribution for all Catalysts: Overall Selectivities ($H_2/CO = 2$, $P = 10.6$ atm, $T = 573$ K)

Catalyst[b]	% Selectivity[a]		
	HC	MeOH	$C_{2+}OH$[c]
Perovskites			
$x = 0.0$	100.0	0.0	0.0
$x = 0.2$	6.3	81.4	11.6
$x = 0.4$	4.0	84.6	9.9
$x = 0.5$	7.0	79.9	9.3
$x = 0.6$	10.2	70.4	18.4
$x = 1.0$	5.7	81.4	12.7
NaO_x/Cu powder	9.1	84.5	5.1
Cu/SiO_2	81.6	4.5	7.2
$La_2O_3/Cu/SiO_2$	34.0	48.7	1.4
Cu/La_2O_3	6.6	78.0	14.4
$Cu/MnO_2/La_2O_3$	5.2	87.7	6.9

[a] Number of C atoms in product/total number of C atoms in all organic products.
[b] F/W as in Tables 3a and 3b.
[c] DME completes the balance in cases where figures do not total 100%.

introduction of copper into the perovskite lattice, the distribution shifts to 90–95% oxygenates. The overall selectivity pattern does not vary widely for $x \geq 0.2$: the selectivity to methanol ranges from 70 to 85%, that to higher alcohols from 9 to 18%, and that to hydrocarbons from 4 to 10%.

For the perovskites, the composition of the higher alcohol fraction is sensitive to the copper content as can be seen from Table 4b. The selectivity to ethanol is lowest for $x = 0.6$. As the selectivity to ethanol decreases, that to isobutanol increases, passing through a maximum at $x = 0.5$. With the exception of $x = 0.2$, *n*-propanol is always present in larger quantities than isopropanol. The combined C_3 alcohol fraction passes through a minimum at $x = 0.6$. For $x = 1$, the ethanol selectivity is higher and the isobutanol selectivity is correspondingly lower than for any of the other perovskites.

It is clear from Tables 4a and 4b, that the product distributions obtained with the lanthana-supported catalysts are similar to those for the perovskites. In particular, the methanol selectivity and the distribution of C_{2+} alcohols observed for Cu/La_2O_3 are almost identical to those for the $x = 0.5$ perovskite, even though the latter catalyst has a higher activity and Cu content. Compared to Cu/La_2O_3, $Cu/MnO_2/La_2O_3$ produces fewer higher alcohols overall and has a slightly higher selectivity to ethanol. The hydrocarbon fractions over both catalysts are essentially the same.

Cu/SiO_2 is >80% selective for the synthesis of hydrocarbons ($\alpha = 0.45$). Small amounts of methanol, ethanol, and dimethyl ether are the only oxygenated products observed. Promotion with lanthana shifts the distribution to nearly 50% methanol and traces of isobutanol. Hydrocarbon production is still prominent but the probability for chain growth, α, decreases to 0.3.

The product distribution for NaO_x/Cu powder is similar to that observed for the perovskites and Cu/La_2O_3. As will be discussed below, this characteristic can be attributed to the promotion of metallic Cu by the basic metal oxide.

TABLE 4b

Product Distribution for all Catalysts: Selectivities among C_{2+} Alcohols ($H_2/CO = 2$, $P = 10.6$ atm, $T = 573$ K)

Catalyst[b]	% Selectivity[a]				
	EtOH	*i*-PrOH	*n*-PrOH	*i*-BuOH	*n*-BuOH
Perovskites					
$x = 0.0$	0.0	0.0	0.0	0.0	0.0
$x = 0.2$	45.2	17.2	14.4	23.1	0.0
$x = 0.4$	25.4	0.6	19.3	54.6	0.0
$x = 0.5$	18.0	1.9	12.4	61.4	6.2
$x = 0.6$	16.2	3.5	12.6	47.7	10.4
$x = 1.0$	50.5	2.6	24.5	18.4	0.0
NaO_x/Cu powder	48.6	10.2	15.7	23.1	0.0
Cu/SiO_2	100.0	0.0	0.0	0.0	0.0
$La_2O_3/Cu/SiO_2$	0.0	0.0	0.0	100.0	0.0
Cu/La_2O_3	20.9	2.5	13.7	62.7	0.0
$Cu/MnO_2/La_2O_3$	54.3	0.0	0.0	45.6	0.0

[a] Number of C atoms in C_{2+} alcohol/total number of C atoms in all C_{2+} alcohols.
[b] F/W as in Tables 3a and b.

Effect of Reaction Conditions on Product Distribution

The influence of temperature on the product distribution is shown in Figs. 4a and 4b for the $x = 0.6$ perovskite. From Fig. 4a it is apparent that the selectivity to methanol falls off with increasing temperature while the selectivities to hydrocarbons and to C_{2+} alcohols both increase. Among the C_{2+} alcohols (Fig. 4b), ethanol and isobutanol are the major products. With increasing temperature, the ethanol selectivity rises monotonically. The selectivity to *n*-propanol, the next most abundant alcohol, passes through a maximum with increasing temperature.

The influence of hydrogen partial pressure is presented in Figs. 5a and 5b. With increasing hydrogen partial pressure the methanol selectivity increases while the selectivity to C_{2+} alcohols decreases. The overall hydrocarbon fraction decreases only slightly and the carbon number distribution shifts toward methane (not shown). Among the C_{2+} alcohols (Fig. 5b) the selectivity to *n*-butanol declines, and the selectivities to the other alcohols, including isobutanol, increase with increasing H_2 partial pressure.

Table 5 summarizes the influence of space velocity on the activity and product distribution for the $x = 0.5$ perovskite. The rate of CO conversion to organic products increases with increasing space velocity. Since the CO conversion is less than 3% in all cases the observed increase in the rate of CO conversion is most likely due to a decrease in product inhibition. The overall selectivity both to hydrocarbons and to higher alcohols increases with decreasing space

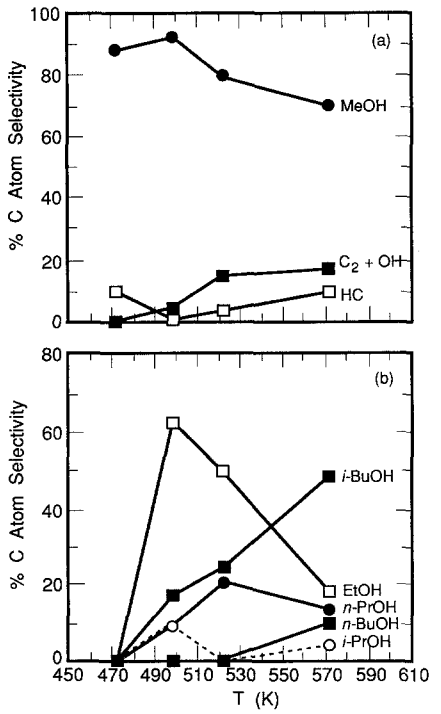

FIG. 4. CO hydrogenation over $LaMn_{0.4}Cu_{0.6}O_3$: effect of temperature on product distribution ($H_2/CO = 2$, $P = 10.6$ atm): (a) overall selectivities, (b) selectivities among C_{2+} alcohols.

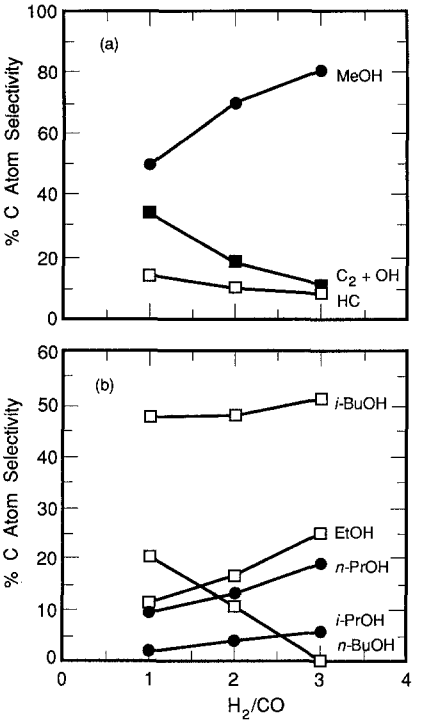

FIG. 5. CO hydrogenation over $LaMn_{0.4}Cu_{0.6}O_3$: effect of hydrogen partial pressure on product distribution ($P_{CO} = 4.2$ atm, $T = 573$ K); (a) overall selectivities, (b) selectivities among C_{2+} alcohols.

TABLE 5

CO Hydrogenation over $LaMn_{0.5}Cu_{0.5}O_3$: Effects of Space Velocity on Activity and Product Distribution ($H_2/CO = 3$, $P = 13.8$ atm, $T = 573$ K)

F/W (ml/min/g catalyst):	222	73	26
CO conversion rate (μmol/min/m^2 catalyst):	2.06	0.61	0.48
Selectivities[a]			
HC	6.4	12.9	18.8
MeOH	76.8	72.1	54.6
C_{2+}OH	8.4	13.1	23.4
Among C_{2+} alcohols			
EtOH	14.4	9.7	4.1
i-PrOH	4.4	12.5	13.6
n-PrOH	10.8	8.0	5.7
i-BuOH	47.0	59.2	65.6
n-BuOH	20.8	0.0	0.0

[a] Selectivities among organic compounds.

velocity. Among the hydrocarbons the average carbon number increases with increasing space velocity (not shown). At lower space velocities the formation of branched C_3 and C_4 alcohols increases at the expense of ethanol.

The effects of reduction temperature on the activity and selectivity of the $x = 0.5$ and $x = 1$ perovskites are presented in Tables 6a and 6b, respectively. For the $x = 0.5$ perovskite, an increase in the reduction temperature causes a decrease in the catalyst activity, a significant decrease in the hydrocarbon selectivity, and a correspond-

TABLE 6a

CO Hydrogenation over $LaCu_{0.5}Mn_{0.5}O_3$: Influence of Reduction Temperature on Activity and Product Distribution[a]

Reduction temperature (K):	523	723
CO conversion rate (μmol CO/min/m^2 catalyst):	0.27	0.16
Cu/La[b]:	0.47	0.46
Selectivity[c]		
HC	12.3	1.91
MeOH	59.9	81.5
C_{2+}OH	25.4	14.4
Among C_{2+} alcohols		
EtOH	37.0	0.0
i-PrOH	6.1	0.0
n-PrOH	2.6	8.9
i-BuOH	47.15	91.6
2-BuOH	5.7	0.0
n-BuOH	1.4	0.0

[a] $H_2/CO = 2$, $P = 10.6$ atm, $T = 573$ K, F/W = 26 ml/min/g catalyst.
[b] Determined by XPS.
[c] Selectivities among organic compounds.

TABLE 6b

CO Hydrogenation over $LaCuO_{2.6}$ (= $La_2CuO_{4+}CuO$): Influence of Reduction Temperature on Activity and Product Distribution[a]

Reduction temperature (K):	523	723
CO conversion rate (μmol CO/min/m^2 catalyst):	1.69	1.83
Cu/La[b]:	0.71	1.11
Selectivity[c]		
HC	5.8	22.8
MeOH	81.5	65.9
C_{2+}OH	12.8	11.2
Among C_{2+} alcohols		
EtOH	50.5	57.2
i-PrOH	2.6	7.3
n-PrOH	24.5	28.9
i-BuOH	18.4	0.0

[a] $H_2/CO = 2$, $P = 10.6$ atm, $T = 573$ K, F/W = 200 ml/min/g catalyst.
[b] Determined by XPS.
[c] Selectivities among organic compounds.

ing increase in the methanol selectivity. While the overall selectivity to higher alcohols is not significantly affected by the catalyst reduction temperature, reduction at 723 K causes the ethanol selectivity to decrease to zero and the isobutanol selectivity to increase. Analysis by XPS of the catalyst used shows no significant change in the Cu/La surface ratios as a function of reduction temperature (see Table 1).

For the $x = 1$ perovskite (Table 6b), the conversion rate for the sample reduced at 723 K is somewhat higher compared to that for the sample reduced at 523 K, and the Cu/La ratio is higher by almost 60%. The increase in overall activity can be traced directly to an increase in the production of hydrocarbons, since the rates of methanol and C_{2+} alcohol formation do not change much with increased reduction temperature. The principal change in the distribution of C_{2+} alcohols is a decrease in the selectivity to isobutanol relative to the C_2 and C_3 alcohols.

Activation Energies

Table 7 lists the apparent activation energies for methane, methanol, and ethanol for temperatures between 473 and 573 K. For other compounds, the yield fell off too rapidly with temperature to provide a suitable Arrhenius plot. The error in the values is $\sim\pm 7\%$.

The activation energies for methane formation over the perovskites, Cu/La_2O_3, $Cu/MnO_2/La_2O_3$, $La_2O_3/Cu/SiO_2$, and NaO_x/Cu all lie in the range 20–25

TABLE 7

Activation Energies

Catalyst	E_a (kcal/mol)		
	CH_4	CH_3OH	C_2H_5OH
Perovskites			
$x = 0.2$	29.7	20.5	2.8
$x = 0.4$	19.8	13.1	7.8
$x = 0.5$	21.9	7.6	10.2
$x = 0.6$	23.2	13.6	19.3
$x = 1.0$	21.8	12.5	10.3
NaO_x/Cu	23.2	18.9	—
Cu/SiO_2	11.4	3.8	—
$La_2O_3/Cu/SiO_2$	21.1	26.4	—
Cu/La_2O_3	22.9	11.9	17.1
$Cu/MnO_2/La_2O_3$	24.9	13.6	—

kcal/mol, but a much lower value of 11.4 kcal/mol is observed for Cu/SiO_2. The activation energies for alcohol synthesis exhibit a much higher sensitivity to catalyst composition than is seen for methane synthesis. The lowest value of the activation energy for methanol synthesis is observed for Cu/SiO_2, 3.8 kcal/mol. When promoted with lanthana the methanol activation energy increases to 26.4 kcal/mol. This trend is similar to that reported recently for lanthana-promoted Rh and Pd catalysts (*33, 34*). The remaining catalysts exhibit activation energies in the range 12–19 kcal/mol, the only exception being the $x = 0.5$ perovskite for which $E_a = 7.6$ kcal/mol. The activation energy for ethanol synthesis over the perovskites ranges from 3 to 19 kcal/mol, passing through this maximum at $x = 0.6$. The ethanol activation energy over Cu/La_2O_3, at 17.1 kcal/mol, also lies in the range spanned by the perovskites.

DISCUSSION

Nature of the Active Copper Species

The results of this study show that $LaMnO_{3.24}$ is not very active for CO hydrogenation and produces hydrocarbons as the only organic product. When Cu is substituted for Mn in the perovskite lattice the CO hydrogenation activity increases monotonically with increasing Cu content and the selectivity switches to ≥80% methanol, independent of the Cu content. These observations are similar to those reported earlier by Broussard and Wade (*22*) and indicate quite clearly the importance of Cu in forming methanol.

It is also significant to note that unpromoted metallic Cu is not particularly active for methanol synthesis. The data in Table 4 demonstrate that Cu/SiO_2 has a methanol selectivity of only 4.5% and that the primary products formed (≈82%) are hydrocarbons. These findings are consistent with the work of Sheffer and King (*18, 19*), who report that for unpromoted Cu powder the CO hydrogenation activity is very low and that the methanol selectivity is 25% (the balance of the products being methane and CO_2). By contrast, when Cu powder is promoted by an alkali-metal oxide, the CO hydrogenation activity of the catalyst increases significantly as does the selectivity to methanol. Thus, both in the present study and in that of Sheffer and King (*19*), NaO_x-promoted Cu exhibits a methanol selectivity of ≥85%. As can be seen from Tables 3a and 4a, promotion of Cu/SiO_2 by La_2O_3 also enhances both the overall CO hydrogenation activity of Cu and the selectivity to methanol.

High CO hydrogenation activity and methanol selectivity are also observed for Cu/La_2O_3 and $Cu/MnO_2/La_2O_3$. What is quite striking is that the activity and selectivities of these catalysts are close to those of the perovskites containing a similar mole fraction of Cu. Table 7 shows that the activation energies for methane formation are also comparable for these catalysts.

The strong similarities between La_2O_3-supported Cu and Cu-containing perovskites suggest that under reaction conditions the state of copper in these catalysts is similar. As discussed under Results, catalyst characterization after use indicates that the La_2O_3-supported catalysts contain fairly large Cu particles ($d \approx 200$ Å) and some ionic Cu stabilized in the oxide lattice. Likewise, the XRD pattern of the $x = 1$ perovskite showed clear evidence for Cu particles. By contrast, neither XRD nor XPS characterization of the perovskite catalysts for which $0.2 \leq x \leq 0.6$ showed any evidence of Cu particles. However, the strong similarity in the product distributions of all the copper-containing perovskites suggests that the $0.2 \leq x \leq 0.6$ perovskites contain very small particles of metallic Cu not detectable by XRD. Thus, in their working state it is envisioned that both La_2O_3-supported Cu and Cu-containing perovskites contain Cu^0 particles as well as ionic forms of copper (viz., Cu^+ and Cu^{2+}). While the catalyst characterization techniques used in this study do not reveal

the spatial relationship between the metallic and ionic forms of copper, as discussed below, previous investigations (*2, 18, 19*) suggest that at least a part of the ionic copper is either on the surface of the Cu^0 particles or in close contact with it.

The formation of hydrocarbons very likely occurs over metallic Cu^0 particles. Since CO will not dissociate over Cu (*35*), the formation of the precursors most likely occurs via the partial hydrogenation of CO to form species such as HCO_s, H_2CO_s, and CH_3O_s, and the subsequent dissociation of these species to form CH_s, CH_{2s}, CH_{3s}, respectively. Theoretical studies by Shustorovich and Bell (*36*) have shown recently that such processes are expected on metals such as Pt and Pd, which, like Cu, contain few *d*-band vacancies.

Previous investigators have proposed that methanol synthesis occurs at Cu^+ sites which may be stabilized in the support or promoter (*2*) or which may exist on the surface of Cu^0 particles modified by adsorption of oxygen or by the presence of an oxidic promoter (e.g., alkali metal oxide) (*6, 18, 19*). The fact that the activity and selectivity of metallic Cu for methanol are enhanced by promotion with either alkali metal or La_2O_3 suggests that Cu particles are required for methanol formation, but that the active sites are most likely Cu^+ (or possibly $Cu^{\delta+}$) ions produced on the surface of these particles through interaction of the promoter with the metal.

The work of Sheffer and King (*19*) with LiCuO suggests that isolated Cu^+ ions are insufficient for methanol synthesis. It was observed that LiCuO is relatively inactive for methanol synthesis until a substantial part of the Cu has been converted under reaction conditions to metallic Cu particles. The necessity for both Cu^0 and Cu^+ is also supported by the observation that the specific activity for methanol formation over alkali-metal oxide-promoted Cu powder increases with increasing Cu^+ concentration (*19*). Similarly, Monnier and co-workers (*37, 38*), in their studies of Cu–Cr oxide catalysts, have shown that while the specific rates of methanol formation were proportional to the amount of Cu^+ (as $CuCrO_2$), the activity was essentially zero in the absence of Cu^0 (i.e., with pure $CuCrO_2$). These authors suggest that Cu^+ enhances the adsorption of CO but that Cu^0 is required for the dissociation of H_2. Similar ideas may also be found in the work of Chinchen *et al.* (*6*) on the effects of adsorbed oxygen on the activity of metallic Cu for CO hydrogenation.

An alternative explanation for the role of oxidic promoters has been offered by Frost (*39*). He proposes that metallic Cu stabilizes cationic oxygen vacancies in regions of the oxide phase that are in contact with the metal, through the formation of Schottky junctions. He proposes a methanol synthesis mechanism in which all the important steps (CO adsorption and hydrogenation) take place at the oxygen vacancies. The only evidence he offers in support of this proposal is that thoria-promoted Ag and Au are active for methanol synthesis whereas the unpromoted metals are not. This is interpreted as promotion of thoria by an otherwise inactive metal, a novel concept. However, in view of the more extensive evidence of Sheffer and King (*18, 19*), Monnier *et al.* (*37, 38*), and Chinchen *et al.* (*6*), it seems more plausible to propose that oxide promoters (i.e., Na_2O, ThO_2, ZrO_2, La_2O_3, etc.) are effective by stabilizing cationic Cu sites on the surface of Cu particles.

Further support for the argument that both Cu^0 and Cu^+ sites are required for methanol synthesis can be drawn from a comparison of the methanol selectivities for Cu/SiO_2, $La_2O_3/Cu/SiO_2$, Cu/La_2O_3, and $LaCuO_{2.6}$. As is seen in Table 4a, the methanol selectivity for these catalysts increases in the order $Cu/SiO_2 < La_2O_3/Cu/SiO_2 < Cu/La_2O_3 \leq LaCuO_{2.6}$. This trend parallels the increasing amount of La_2O_3 present in the catalyst. Since XRD characterization of

the catalysts used clearly shows evidence of Cu particles ($d \geq 100$ Å) in all these catalysts, the higher selectivity can be attributed to the increased stabilization of Cu^+ ions by La_2O_3. It is interesting to recall here that Sheffer and King (*19*) have observed increases in both the activity and the selectivity of alkali-promoted Cu with increasing surface concentration of Cu^+.

Features of the Product Distribution

The data presented in Table 4b indicate that the principal components of the C_{2+} alcohols produced over copper catalysts containing lanthana (or soda) are ethanol, *n*-propanol, and isobutanol. Modest proportions of isopropanol and *n*-butanol are occasionally observed. This distribution for C_{2+} alcohols is similar to that observed for alkali-promoted Cu/ZnO by Vedage *et al.* (*10*) and more recently by Nunan *et al.* (*40*). In both reports it was proposed that one of the roles of the basic metal oxide promoter is to stabilize the presence of oxygen-containing surface species which are considered to be intermediates in the formation of higher alcohols.

To elucidate the reaction pathways by which C_{2+} alcohols are formed, Nunan *et al.* (*40*) carried out extensive isotopic tracer studies with Cs-promoted Cu/ZnO. Based on the product distribution observed upon injection of ^{13}C-labelled alcohols into the feed, they concluded that the formation of higher alcohols occurs primarily by the addition of C_1 intermediates derived from methanol (i.e., HCO^- or H_2CO). Two major routes for chain growth were proposed. The first, termed linear chain growth (l), involves the nucleophilic attack at the α-carbon of an adsorbed aldehydic or alcohol intermediate by formyl (HCO^-). These processes are illustrated by the reactions (where B^+) is a basic cation, e.g., Cs^+, etc.):

$$R\text{—}CH\text{=}O + HCO\text{—}B^+ = R\text{—}\underset{\displaystyle O\text{—}B^+}{\overset{\displaystyle |}{CH}}CH\text{=}O \qquad (1)$$

$$R\text{—}CH_2OH + HCO^- B^+ = R\text{—}CH_2CH\text{=}O + OH^-B^+. \qquad (2)$$

Hydrogenation of the products of these reactions leads to the formation of a linear primary C_{2+} alcohol. The formation of a linear secondary alcohol can also be envisioned if, during the hydrogenation of the product of reaction (1), the aldehydic oxygen is removed. Nunan *et al.* (*40*) indicate, however, that the formation of secondary alcohols is less favorable than the formation of primary alcohols.

The second major pathway for chain growth is termed β-addition and is thought to proceed as follows:

$$RCH_2CH_2OH = R\text{—}CH_2CH\text{=}O \qquad (3)$$

$$R\text{—}CH_2CH\text{=}O + B^+ OH^- = R\text{—}\underset{\displaystyle B^+}{\overset{\displaystyle |}{CH}}\text{=}CHO^- + H_2O \qquad (4)$$

$$R\text{—}\underset{\displaystyle B^+}{\overset{\displaystyle |}{CH}}\text{=}CHO^- + H_2C\text{=}O = HCC(R)HCH\text{=}O. \qquad (5)$$

Subsequent reactions (hydrogenation, dehydration, and hydrolysis) result in the formation of a branched primary alcohol. As with α-addition, Nunan *et al.* (*40*) indicate that the preferred pathway in β-addition involves retention of the aldehydic oxygen. They refer to the overall process of β-addition as aldol coupling with oxygen retention reversal, since in normal aldol condensation reactions, the oxygen atom is removed from the added aldehyde group (*41*).

Nunan *et al.* (*40*) have also proposed that the mechanisms for producing C_{2+} alcohols over Cu/ZnO and Cs/Cu/ZnO catalysts are similar. They ascribe the enhanced selectivity to C_{2+} alcohols and the preferential formation of branched alcohols over Cs/Cu/ZnO to Cs promotion of the rates of α- and β-addition, in particular the latter process.

Since lanthana is a highly basic metal oxide (*42*), its effects on the synthesis of C_{2+} alcohols over Cu are expected to be similar to those of Cs. In particular we note that while ethanol is the only higher alcohol observed over Cu/SiO_2, isobutanol is the major higher alcohol formed when this catalyst is promoted with La_2O_3. This effect can be attributed to enhancement by lanthana of chain growth by β-addition. Also in agreement with the mechanism proposed by Nunan *et al.* (*40*) are the effects of space velocity shown in Table 6. It is evident that the proportion of C_{2+} alcohols increases with decreasing space velocity. This trend can be ascribed to more extensive chain growth at longer residence times, due to the higher concentration of methanol over the catalyst. A higher concentration of gas-phase methanol would be expected to increase the concentration of adsorbed methanol, as well as the concentrations of adsorbed formaldehyde and formyl species derived from methanol via dehydrogenation. Low H_2/CO ratios should also favor increased surface concentrations of these partially hydrogenated species and hence the increase in selectivity to C_{2+} alcohols, shown in Figs. 5a and 5b.

Effects of Manganese on Catalyst Performance

The effects of MnO_2 on the activity and selectivity of Cu are best judged by comparing the characteristics of Cu/La_2O_3 and $Cu/MnO_2/La_2O_3$. The data in Table 3a indicate that $Cu/MnO_2/La_2O_3$ is less active than Cu/La_2O_3. Since both catalysts contain the same amount of Cu, the lower activity of $Cu/MnO_2/La_2O_3$ may reflect the lower dispersion of the catalyst (see Table 1). Table 4a shows that the presence of MnO_2 increases the selectivity to methanol, primarily at the expense of the C_{2+} alcohol selectivity. The distribution of C_{2+} alcohols shift toward a lower carbon number. In fact, under the conditions given in Table 3a, only ethanol and isobutanol are observed: it was not possible to detect the presence of propanols.

CONCLUSIONS

This study has revealed a number of interesting features of CO hydrogenation over catalysts containing copper, lanthanum, and manganese. $LaMnO_{3.24}$ is found to be relatively inactive and to produce hydrocarbons with 100% selectivity. Substitution of copper for manganese in the lattice of the perovskite results in a significant increase in CO hydrogenation activity and a switch to production of methanol (~80% selectivity) and C_{2+} alcohols (~10% selectivity). CO hydrogenation over metallic copper produces hydrocarbons with high selectivity (~80%) and small proportions of methanol and C_{2+} alcohols. Promotion of copper with lanthana or use of lanthana as a support results in a significant increase in the activity and an increase in the selectivity to methanol and C_{2+} alcohols. NaO_x-promotion of metallic copper has an effect similar to that produced by lanthana.

The strong similarities observed in the activity and selectivities of the copper-containing perovskite catalysts, $La_2O_3/Cu/SiO_2$ and Cu/La_2O_3, suggest that the active

sites in all of the catalysts are similar. On the basis of the results of catalyst characterization and earlier published studies of alkali-promoted copper, it is proposed that hydrocarbon synthesis occurs at Cu^0 sites, but that Cu^0 and Cu^+ sites are required for the formation of methanol and C_{2+} alcohols. It is proposed that Cu^+ can be stabilized at the adlineation between metallic copper and La_2O_3 (or NaO_x). Manganese present as a part of the perovskite lattice or dispersed as MnO_2 on La_2O_3 does not appear to have a strong influence on the activity of copper catalysts for CO hydrogenation, but does suppress the formation of C_{2+} alcohols somewhat.

ACKNOWLEDGMENTS

This work was supported by the Division of Chemical Sciences, Office of Basic Energy Research, U.S. Department of Energy, under Contract DE-AC03-76SF00098, and by the Spanish–North American Joint Committee for Scientific and Technological Cooperation, under Grant CCB-8409/003.

REFERENCES

1. (*a*) Davies, P., Snowdon, F. F., Bridger, G. W., Hughes, D. O., and Young, P. W., U.K. Patent 1,010,871 (to ICI). (*b*) Gallagher, J. T., and Kidd, J. M., U.K. Patent 1,159,035 (to ICI). (*c*) Cornthwaite, D., U.K. Patent 1,296,212 (to ICI).
2. Herman, R. G., Klier, K., Simmons, G. W., Finn, B. P., Bulko, J. B., and Kobylinski, T. P., *J. Catal.* **56,** 407 (1979).
3. Klier, K., Chatikavanij, V., Herman, R. G., and Simmons, G. W., *J. Catal.* **74,** 343 (1982).
4. Chinchen, G. C., Waugh, K. C., and Whan, D. A., *Appl. Catal.* **25,** 101 (1986).
5. Pan, W. X., Cao, R., Roberts, D. L., and Griffin, G. L., *J. Catal.* **114,** 440 (1988).
6. Chinchen, G. C., Spencer, M. S., Waugh, K. C., and Whan, D. A., *J. Chem. Soc. Faraday Trans. 1* **83,** 2193 (1987).
7. Chinchen, G. C., Plant, C., Spencer, M. S., and Whan, D. A., *Surf. Sci. Lett.* **184,** L370 (1987).
8. Chinchen, G. C., Denny, P. J., Parker, D. G., Spencer, M. S., and Whan, D. A., *Appl. Catal.* **30,** 333 (1987).
9. Natta, G., Colombo, U., and Pasquon, I., *in* "Catalysis" (P. H. Emmet, Ed.), Vol. V, pp. 131–174. Reinhold, New York, 1957.
10. Vedage, G. A., Himelfarb, P., Simmons, G. W., and Klier, K., *Amer. Chem. Soc. Prepr. Div. Petrol. Chem.* **28**(5), 1261 (1983).
11. Smith, K. J., and Anderson, R. B., *J. Catal.* **85,** 428 (1984).
12. Hofstadt, C. E., Schneider, M., Bock, O., and Kochloefl, K., in Poncelet, G., Grange, P., and Jacobs, P. A. (Eds.), "Preparation of Catalysts III," pp. 709–721. Elsevier, Amsterdam, 1987.
13. Nunan, J., Klier, K., Young, C.-W., Himelfarb, P. B., and Herman, R. G., *J. Chem. Soc. Chem. Commun.*, 193 (1986).
14. Chen, B., Zhao, J., Zhu, C., Ma, F., and Kang, H., *Zhongguo Xito Xuebao* **5**(1), 43 (1987).
15. Liu, J., and Liu, D., *in* "Proceedings, 3rd China–Japan–U.S. Symposium on Catalysis, Xiamen, People's Republic of China," Poster C-05 (1987).
16. Owen, G., Hawkes, C. M., Lloyd, O., Jennings, J. R., Lambert, R. M., and Nix, R. M., *Appl. Catal.* **33,** 405 (1987).
17. Nix, R. M., Judd, R. W., Lambert, R. M., Jennings, R. M., and Owen, G., *J. Catal.* **118,** 175 (1989).
18. Sheffer, G. R., and King, T. S., *J. Catal.* **115,** 376 (1989).
19. Sheffer, G. R., and King, T. S., *J. Catal.* **116,** 488 (1989).
20. Klier, K., Herman, R. G., and Young, C.-W., *Amer. Chem. Soc. Prepr. Div. Fuel Chem.* **29**(5), 273 (1984).
21. Xiaoding, X., Doesburg, E. B. M., and Scholten, J. J. F., *Catal. Today* **2,** 125 (1987).
22. Broussard, J. A., and Wade, L. E., *Amer. Chem. Soc. Div. Fuel Chem. Prep. Pap.* **31**(3), 75 (1986).
23. Rojas, M. L., Fierro, J. L. G., Tejuca, T. G., and Bell, A. T., *J. Catal.* **124,** 41 (1990).
24. Tascón, J. M. D., Mendioroz, S., and Tejuca, L. G., *Z. Phys. Chem. N.F.* **124,** 109 (1981).
25. Rosynek, M. P., and Magnuson, D. T., *J. Catal.* **46,** 402 (1977).
26. Underwood, R. P., and Bell, A. T., *Appl. Catal.* **21,** 157 (1986).
27. Wagner, C. D., Riggs, W. M., Davis, L. E., Moulder, J. F., and Muilenberg, G. E. (Ed.), "Handbook of X-Ray Photoelectron Spectroscopy," Perkin–Elmer Corp., Physical Electronics Division, Eden Prairie, 1976.
28. Parris, G. E., and Klier, K., *J. Catal.* **97,** 374 (1986).
29. Scholten, J. J. F., and Konvalinka, J. A., *Trans. Faraday Soc.* **65,** 2465 (1969).
30. Dell, R. M., Stone, F. S., and Tiley, P. F., *Trans. Faraday Soc.* **49,** 195 (1953).
31. Demazean, G., Parent, C., Pouchard, M., and Hagenmuller, P., *Mater. Res. Bull.* **7,** 913 (1972).
32. Hicks, R. F., Yen, Q. J., and Bell, A. T., *Appl. Surf. Sci.* **19,** 315 (1984).
33. Hicks, R. F., and Bell, A. T., *J. Catal.* **91,** 104 (1985).
34. Underwood, R. P., and Bell, A. T., *J. Catal.* **111,** 325 (1988).

35. Brodén, G., Rhodin, T. N., Brucker, C., Brendow, R., and Hurych, Z., *Surf. Sci.* **59,** 593 (1976).

36. Shustorovich, E., and Bell, A. T., *J. Catal.* **113,** 341 (1988).

37. Monnier, J. R., and Apai, G., *Amer. Chem. Soc. Div. Fuel Chem. Prep. Pap.* **31**(6), 239 (1986).

38. Apai, G., Monnier, J. R., and Hanrahan, M. J., *J. Chem. Soc. Chem. Commun.,* 212 (1984).

39. Frost, J. C., *Nature (London)* **334,** 577 (1988).

40. Nunan, J. G., Bogdan, C. E., Klier, K., Smith, K. J., Young, C.-W., and Herman, R. G., *J. Catal.* **116,** 195 (1989).

41. Morrison, R. T., and Boyd, R. N., "Organic Chemistry," 4th ed., p. 867. Allyn & Bacon, Boston, 1983.

42. Moeller, T., "Chemistry of the Lanthanides," p. 24. Reinhold, New York, 1963.